Available online at www.sciencedirect.com
SCIENCE DIRECT
Applied Catalysis A: General 283 (2005) 91–98
APPLIED CATALYSIS A: GENERAL
www.elsevier.com/locate/apcata

The role of vanadium on the properties of iron based catalysts for the water gas shift reaction

Ivan Lima Júnior[a], Jean-Marc M. Millet[b], Mimoun Aouine[b], Maria do Carmo Rangel[a,*]

[a]*Instituto de Química, Universidade Federal da Bahia, Campus Universitário de Ondina, Federação, 40290-170 Salvador, Bahia, Brazil*
[b]*Institut de Recherches sur la Catalyse, 2 Avenue Albert Einstein, F 69626 Villeurbanne Cedex, France*

Received 14 August 2004; received in revised form 28 December 2004; accepted 28 December 2004
Available online 26 January 2005

Abstract

The substitution of chromium by vanadium as dopant in the iron oxide based water gas shift (WGS) catalyst has been investigated. Catalysts prepared as magnetite with different amount of vanadium have been prepared and tested with different amounts of water in the gas feed. The results obtained showed that vanadium was a promising dopant leading to very active and stable catalysts. The vanadium-doped catalysts have been characterized by means of chemical analysis, X-ray diffraction, Fourier transform infrared spectroscopy, specific surface area measurements, temperature-programmed reduction, Mössbauer spectroscopy, X-ray photoelectron spectroscopy and high resolution transmission electron microscopy with electron diffraction. Vanadium has been shown to be present both as V(III) and V(IV) species at the surface and in the bulk near the surface of the magnetite structure. It increased the specific surface area of the catalysts and kept the particles apart on the surface delaying sintering. The vanadium doping has been shown to have also an effect on the Fe(III) content of the magnetite which increased favoring the successive oxidation and reduction cycles, during the reaction.

Keywords: Magnetite; Hydrogen; WGSR; Vanadium; Iron oxide

1. Introduction

The demand for high-purity hydrogen for industrial application is today largely met by the water gas shift reaction (WGSR). In some applications, like the manufacture of ammonia or the production of synthesis gas, hydrogen is primarily obtained from the reforming of methane or higher hydrocarbons, a reaction that produces carbon monoxide and hydrogen as main products. However, the hydrogen concentration obtained is not sufficient for the applications cited above and the WGSR has to be used to maximize the hydrogen production. The reaction presents the advantage of simultaneously reducing the carbon oxides to a very low level and thus avoiding the poisoning of the ammonia-synthesis catalysts as well as of most of the metallic hydrogenation catalysts [1,2].

In order to achieve rates for commercial purposes, the WGSR is performed in two steps, successively at high temperature (623–723 K) and at low temperature (453–523 K) [1,3,4]. The first step involves an iron and chromium-based catalyst, which decreases the carbon monoxide concentration from ca. 10 mol% (for natural gas derived synthesis gas) to ca. 3 mol% in kinetic favorable conditions. In the second step, the carbon monoxide concentration is further decreased to ca. 0.3 mol%, using a copper zinc oxide based catalyst in thermodynamic favorable conditions [1,3].

The classical industrial high temperature shift (HTS) catalysts contain iron oxide as well as chromium oxide which is believed to act as a stabilizer, retarding sintering and avoiding the loss of specific surface area [1–3]. It contains 92% by weight of hematite (α-Fe_2O_3) and 8% by weight of chromium oxide (Cr_2O_3), whereby the components may be prepared by several routes separately or together [5]. Before the HTS catalysts can be used hematite must be converted to magnetite (Fe_3O_4), which is believed to be the active phase. This reduction is carried out with the

* Corresponding author. Tel.: +55 71 237 5784; fax: +55 71 235 5166.
E-mail addresses: jean-marc.millet@catalyse.cnrs.fr (J.M. Millet), mcarmov@ufba.br (M. do Carmo Rangel).

0926-860X/$ – see front matter © 2005 Elsevier B.V. All rights reserved.
doi:10.1016/j.apcata.2004.12.038

process gas (a mixture with composition around 10% CO, 10% CO_2, 60% H_2 and 20% N_2) and is controlled to avoid the further reduction of magnetite to metallic iron, which would promote undesirable reactions like methanation and carbon monoxide disproportionation [1,2]. In order to ensure the magnetite stability in industrial processes, large amounts of steam are added to the gas feeds, which drastically increase the operational costs. There is thus the need to develop more stable catalysts that would not need too much water and that would be more difficulty to reduce to metallic iron [2]. With that respect, the development of a catalyst directly in magnetite form may increase the process efficiency not only because of the energy saved but also due to the gain in life-time of the catalyst that could be expected. This work, which has been undertaken as a part of a general study of the development of such catalysts, deals with the use of several dopants instead of chromium in HTS catalysts produced directly as magnetite [6–10].

In previous works it has been noted that magnetite can be conveniently obtained by heating iron(III)hydroxoacetate (IHA) under nitrogen [6,10], providing an inexpensive and reliable route for this oxide for industrial applications. In the present work, the production of vanadium-doped magnetite by heating vanadium-doped IHA was described. Different vanadium containing catalysts have been prepared and characterized by means of chemical analysis, X-ray diffraction, Fourier transform infrared spectroscopy, specific surface area measurements, temperature-programmed reduction, Mössbauer spectroscopy, X-ray photoelectron spectroscopy and high resolution transmission electron microscopy with electron diffraction. The catalysts were tested in a microreactor in the HTS reaction.

2. Experimental

Reagents used were analytical grade. In sample preparation a 0.25 M nitric acid aqueous solution was slowly added to an ammonium metavanadate one (0.025 M) at room temperature. The subsequent addition of a concentrated ammonium hydroxide (25%) led to an orange solution indicating the presence of the VO_4^{3-} ion. The resulting solution was mixed with an iron nitrate solution (1 M) and kept under stirring for 1 h at room temperature. The final pH was 10. The sol was centrifuged, washed with a 5% (w/v) ammonium acetate solution and centrifuged again. This procedure was repeated until no nitrate ion was detected anymore. The qualitative analysis of nitrate was performed by adding about 1 ml of concentrated sulfuric acid to 10 ml of supernatant, after each centrifugation [11]. The gel was dried in an oven at 393 K, sieved in 100 mesh and then heated at 673 K for 2 h, under nitrogen (100 ml/min). This procedure produced the V10 sample (V/Fe (molar) = 0.1). The method described was repeated using a 0.008 M solution of ammonium metavanadate to get a sample with a V/Fe = 0.03 (V3 sample). A sample without vanadium was also prepared by the same method (I sample). The solids thus obtained were characterized by several techniques and without any pretreatment.

In order to determine their iron content, the solids were dissolved in concentrated hydrochloric acid, under reflux for 10 min in a carbon dioxide atmosphere. After reduction of the Fe(III) to Fe(II) with stannous chloride, the solution was titrated with potassium dichromate [11]. The analysis of the Fe(II) content was carried out on fresh and on spent catalysts to follow the magnetite formation and its stability under the reaction atmosphere. The amount of vanadium in the solids was determined by inductively coupled plasma atomic emission spectroscopy (ICP/AES), using an ARL model 3410 equipment. Carbon analyses were carried out using a LECO model 761-100 apparatus.

Fourier transform infrared spectroscopy (FTIR) was used to confirm the presence of acetate species in solids. The experiments were carried out by means of a Jasco model Valor-III equipment in a range of 400–4000 cm^{-1} using KBr discs. X-ray diffractograms were taken at room temperature in a Rigaku Miniflex model instrument using Cu Kα radiation.

The specific surface areas were measured by using the BET nitrogen adsorption method. The catalyst (0.20 g) was heated for 1 h under flowing nitrogen at 423 K and then analyzed in a Micromeritics TPD/TPO 2900 model equipment, using a 30% N_2/He mixture. The TPR profiles were recorded in the same equipment, using 0.35 g of the sample and following the hydrogen consumption from a 5% H_2/N_2 mixture in the range of 298–1273 K.

The Mössbauer spectra were recorded at room temperature, using a 2 GBq ^{57}Co/Rh source and a conventional constant acceleration spectrometer, operating in triangular mode. The samples were diluted into alumina in order to avoid a too high Mössbauer absorption, and pressed into pellets. The isomer shifts (δ) were given with respect to α-Fe and were calculated, as the quadrupole splittings (Δ), with a precision of about 0.03 mm s^{-1}. The validity of the computed fits was judged on the basis of both χ^2 values and convergences of the fitting processes. All the fits have been achieved using sextuplets without fixing any parameters. The relative ratio of the magnetite sites (A and B) has been calculated using the relative spectral surface areas and considering a f_a/f_b ratio determined by Häggström et al. equal to 1.25 [12].

The recording of the high resolution transmission electron micrographs (HRTEM) and electron diffractograms were carried out using a JEOL 2010 equipment operating at 200 kV with a high resolution pole piece and an energy dispersive x-ray spectrometer (EDS) (Link Isis from Oxford Instruments). The samples were dispersed in ethanol using a sonicator and a drop of the suspension was dripped onto a carbon film supported on a copper grid and then ethanol was quickly evaporated. EDS study was carried out using a probe size of 15 nm to analyze borders and centers of the particles

and the small particles. Standard deviations were evaluated for atomic ratio from at least 10 analyzes.

X-ray photoelectron spectra (XPS) were recorded in a VG ESCALAB 200R spectrometer equipped with an Al Kα X-ray radiation source ($h\nu$ = 1486.6 eV) and a hemispherical electron analyzer. Binding energies were corrected relative to the carbon 1s signal at 284.6 eV. The experimental precision on quantitative measurements was considered to be around 10%. The spectra of the spent catalysts have been recorded after quenching from the reaction temperature and transfer under ambient air in the XPS apparatus.

In order to evaluate the performance of the catalysts, 0.2 cm^3 of powder within −250 and +325 mesh size was used in a fixed bed microreactor consisting of a stainless tube. All experiments were carried out under isothermal conditions (643 K) and at atmospheric pressure, providing there was no diffusion effect. A gas feed with composition 10% CO, 10% CO_2, 60% H_2 and 20% N_2 (process gas) was used. Two values of steam to process gas molar ratio were used: S/G = 0.6 (used in industrial plants) and S/G = 0.2 (to minimize the steam consumption). The gaseous effluent was analyzed by on line gas chromatography, using a CG model 35 instrument, with a thermal conductivity detector (at 373 K) and a 13X sieve molecular column (2 m, 1/8″), at 313 K using hydrogen as carrier (30 ml/min). The reaction was monitored by measuring the carbon monoxide and dioxide concentration in the stream for 6 h. A commercial catalyst, based on iron and chromium, was used to compare the performance of the solids produced.

In order to determine the role of vanadium in these catalysts, a mechanical mixture of the pure iron oxide (I sample) and vanadium oxide (V_2O_5) in a molar ratio of 10, and a pure vanadium oxide were also evaluated in the HTS reaction.

Samples similar to spent catalysts were produced by heating the solids, under flowing process gas, at 643 K for 6 h, using the same values of steam to gas molar ratio of the catalytic tests. These samples were analyzed in terms of Fe(II)/Fe(III) ratio and characterized by X-ray diffraction, specific surface area measurement, Mössbauer spectroscopy, XPS and HRTEM.

3. Results and discussion

The X-ray diffractograms of the fresh catalysts all showed the pattern of magnetite as illustrated in Fig. 1 [13]. No other phase was detected. The interplanar spacing (Table 1) did not change due to vanadium, which might suggest that it did not enter the magnetite lattice. However, by considering the tendency of magnetite of accepting foreign species in its structure [14], as well as the Goldschmidt rules [15], it is more probable that vanadium goes into solution with the iron oxide, rather than it remains as vanadium oxide (V_2O_5). The interplanar spacings did not

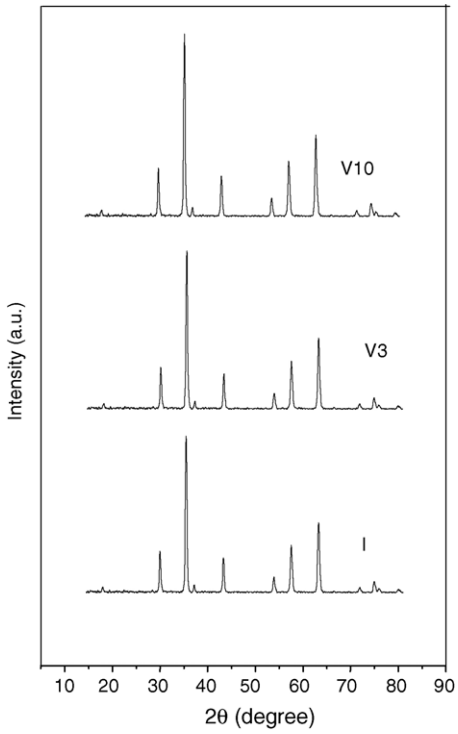

Fig. 1. X-ray diffractograms of magnetite (I sample) and vanadium-doped magnetite (V3 sample: V/Fe = 0.03; V10 sample: V/Fe = 0.10).

change probably due to the low amounts of vanadium incorporated and to almost the same values of cationic radii for V and Fe [16]. After the catalytic tests, the samples showed the same diffraction pattern as the fresh catalysts, regardless the steam to gas ratio.

The elemental analysis results are presented in Table 2. It can be noted that vanadium did not affect the magnetite production, since all samples showed a Fe(II)/Fe(III) ratio near the stoichiometric value of magnetite (0.5). The ratios calculated for the spent catalysts were similar, which shows that the catalysts were stable under the reaction atmosphere. The carbon contents remained in values below 0.3% and are not supposed to damage the catalyst but rather aid its pelletization [17].

The Mössbauer spectra of the fresh catalysts (Fig. 2) showed that the introduction of vanadium cations in the material led to a solid relatively oxidized with a structure

Table 1
Interplanar spacings (d) of pure magnetite (I sample) and vanadium-doped magnetite (V3 sample: with V/Fe = 0.03; V10 sample: with V/Fe = 0.1)

d (Å) Magnetite [14]	d (Å) (±0.02) I sample	d (Å) (±0.02) V3 sample	d (Å) (±0.02) V10 sample
2.9673	2.97	2.99	2.99
2.5305	2.52	2.54	2.54
2.082	2.08	2.10	2.10
1.7132	–	1.71	1.71
1.6152	1.60	1.62	1.62
1.4836	1.47	1.49	1.50
1.2799	1.28	1.28	–
1.2114	–	–	1.20

Table 2
Elemental analysis results of pure iron oxide (I sample) and vanadium-doped iron oxide (V3 sample: with V/Fe = 0.03; V10 sample: V/Fe = 0.1)

Sample	% Fe (±0.2)	% Fe(II) (±0.2)	% V (±0.04)	% C (±0.2)	Fe(II)/Fe(III) (atomic)	V/Fe (atomic)
I	83.9	28.7	–	0.3	0.52	–
V3	81.6	26.1	1.96	0.3	0.47	0.026
V10	82.0	27.0	4.15	0.3	0.49	0.055

corresponding to magnetite. Table 3 gathers the Mössbauer parameters of the V3 samples before and after the reaction. At room temperature, the spectra were characterized by two Fe(III) sites and 2–3 Fe(II/III) sites accordingly to previous published studies on substituted magnetite [18]. The Fe(III) site with the smaller isomer shift has been ascribed to Fe(III) (A) and the other to Fe(III) (B). It can be noted that the relative ratios of the A to B sites was close to 1/2 which confirms the presence of vanadium in solids, occupying the B sites [19]. The values of the Fe(III) sites observed ($\delta = 0.36$ mm s^{-1}) were in good agreement with those generally measured ($\delta = 0.38 \pm 0.03$ mm s^{-1}) [19]. Considering the typical value of ($\delta = 0.96 \pm 0.04$ mm s^{-1}) measured for the Fe(II) (B) and that the mean charge of each B site was proportional to δ, the mean charge V_m of the Fe(III/II) species were calculated. We can observe that these values were close or slightly superior to 2.3. The lines width of the B sites were larger than those of the A sites, indicating a range of electronic environments probably related to the presence of vanadium cations. It could be noted that the site with the larger width in V3 sample was the site with lower internal magnetic field and the smaller charge, which could well fitted with a distribution of sextets than only one.

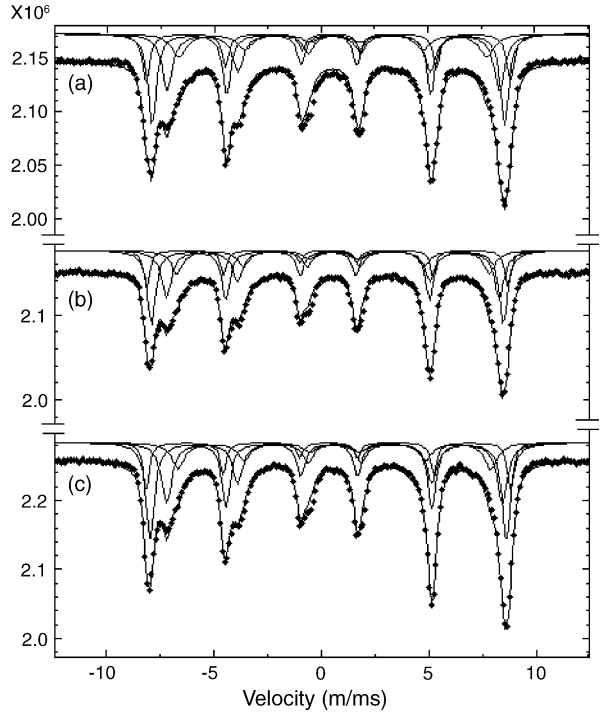

Fig. 2. Mössbauer spectra of the V3 sample (vanadium-doped sample with V/Fe = 0.03) (a) before the HTS reaction and after the reaction carried out under a steam to process gas molar ratio of 0.2 (b) and 0.6 (c).

The V10 sample could be fitted the same way the V3 sample. However, it could be observed that the sextet with the larger internal field was characterized by a slightly negative quadrupolar splitting characteristic of hematite and should thus be attributed to this phase (Table 3). If we consider in a first approximation that the Lamb-Mössbauer factors of magnetite and hematite are equal we can see that 17% of the iron cations are in the hematite type phase. The Fe(III) (A) and Fe(III) (B) of the magnetite type phase could not be well separated in this case and should correspond to the same sextet. It is interesting to note that the magnetite phase in V10 was less oxidized than in V3. This could be in agreement with the increase in relative amount of the doping cations with a larger charge.

After the catalytic tests the Mössbauer spectra showed that, in the V3 sample, the relative amount of Fe(III) has decreased although the mean charge of the Fe(II/III) sites did not vary too much. This reduction was amplified when the amount of steam was larger. Such result was predictable since it is known that the reduction of this type of solid is catalyzed by surface hydration [20]. In the V10 spectrum, the hematite sextet was not observed anymore and the spectra could be fitted with the same four sextets as before. It could be noted that the calculated relative amount of the A sites was slightly lower that the theoretical one which could indicate that vanadium cations could also be present in the A site. Like for the V3 sample, the V10 catalyst was reduced after the catalytic test.

The specific surface areas of the fresh catalysts are shown in Table 4. It can be noted that vanadium-doped samples showed higher values than pure magnetite independently from the vanadium contents in the solids, since the values differ more than 10%. It was not found any significant change in the values of the spent catalysts, as compared to the fresh ones, showing that all solids were stable under the reaction atmosphere. It is known that the steam favors sintering of the HTS catalysts [21]. However, it can be noted that even in the experiments carried out with a steam to gas ratio equal to 0.6, the amount of vapor was insufficient to cause a significant decrease of the specific surface areas. It can be concluded that the catalyst prepared in active form (magnetite) is stable under the reaction condition regardless the presence of vanadium and the presence of steam.

The catalysts have been characterized by XPS before and after the catalytic reaction. Iron, vanadium and oxygen were analyzed. The iron species were identified by a peak at around 710.9 eV, which is characteristic of magnetite [22]. The V2p$_{3/2}$ core-level spectrum showed a peak at around 516.1 eV which can be deconvaluated into two peaks at 516.5 and 516.1 eV, respectively assigned to V(III) and V(IV).

Table 3
Mössbauer parameters computed from the spectrum of the V3 samples, recorded at 295 K and fitted to four doublets

Sample	Site	δ	Δ (mm s^{-1})	H (kOe)	V_m	Rel. intensity (%)
V3	Fe(III) (B)	0.36	0.00	505		33
	Fe(III) (A)	0.36	0.00	492		34
	Fe(III/II) (B)	0.42	0.00	474	2.90	7
	Fe(III/II) (B)	0.56	0.00	452	2.66	12
	Fe(III/II) (B)	0.61	−0.12	407	2.58	14
V3 SG 0.2	Fe(III) (B)	0.38	0.00	509		25
	Fe(III) (A)	0.34	0.00	494		33
	Fe(III/II) (B)	0.66	0.00	462	2.50	35
	Fe(III/II) (B)	0.62	−0.08	430	2.56	7
V3 SG 0.6	Fe(III) (B)	0.39	0.00	506		10
	Fe(III) (A)	0.32	0.00	492		34
	Fe(III/II) (B)	0.67	0.00	460	2.48	41
	Fe(III/II) (B)	0.55	0.00	426	2.68	10
V10	Fe(III) (C)	0.40	−0.15	504		18
	Fe(III) (A + B)	0.35	0.00	487		29 (35)
	Fe(III/II) (B)	0.60	0.00	459	2.60	35 (43)
	Fe(III/II) (B)	0.58	0.00	425	2.63	18 (22)
V10 SG 0.2	Fe(III) (B)	0.37	0.00	498		15
	Fe(III) (A)	0.35	0.00	484		31
	Fe(III/II) (B)	0.62	0.00	458	2.57	33
	Fe(III/II) (B)	0.63	0.00	430	2.55	20
V10 SG 0.6	Fe(III) (C)	0.39	0.00	506		11
	Fe(III) (A)	0.32	0.00	492		29
	Fe(III/II) (B)	0.67	0.00	460	2.48	48
	Fe(III/II) (B)	0.55	0.00	426	2.68	12

δ: isomer shift, Δ: quadrupolar splitting, H: internal magnetic field, V_m: calculated mean charge. Relative proportions of the species in the magnetite like structure are given in the parenthesis for the V10 compound which contained ferric oxide.

The fresh V10 sample showed a lower V(IV)/V(III) ratio (1.1) than the spent one (2.0). The surface V/Fe ratio of the fresh catalyst calculated from the XPS data (V/Fe = 0.26) is higher than the bulk one determined by ICP/AES (V/Fe = 0.055). This clearly shows that the surface of the solids is richer in vanadium than the bulk. Furthermore, this ratio increased after the catalytic test (V/Fe = 0.34) showing that a diffusion of vanadium from the bulk to the surface occurred in the conditions of catalysis. This diffusion should lead at the reduced surface to the substitution mechanism:

$$O^{2-} + 2Fe^{3+} \leftrightarrows \square_O V^{4+} + \square_C \quad (1)$$

where $\square_O$ and $\square_O$ stand, respectively for an anionic and a cationic vacancy. This diffusion process should take place at the same time as the reduction of iron:

$$O^{2-} + 2Fe^{3+} \leftrightarrows 2Fe^{2+} + \square_O \quad (2)$$

It should limit the reduction of iron and therefore stabilize the magnetite in the conditions of catalytic reaction.

Table 4
Specific surface area (S_g) of pure magnetite (I sample) and of vanadium-doped magnetite (V3 sample: V/Fe = 0.03; V10 sample: V/Fe = 0.1) before and after the HTS reaction

Sample	S_g (m^2 g^{-1}) fresh catalyst	S_g (m^2 g^{-1}) spent catalyst S/G = 0.6	S_g (m^2 g^{-1}) spent catalyst S/G = 0.2
I	19	21	20
V3	25	28	26
V10	27	28	28

Fig. 3 shows the results of a HRTEM investigation of the V10 catalyst before and after the catalyst test. The solids presented particles of different shapes and sizes in the range of 10–100 nm (Fig. 3a). These particles were well crystallized and all their electron diffraction patterns corresponded to magnetite. After the catalytic test the particles appeared slightly bigger and more rounded. In Fig. 3b, it can be seen that some of them have a tendency to form necks with each other showing that a sinterization process occurred. However, such process should have been rather limited since it did not significantly change the specific surface areas as shown in Table 4. The EDX analyses of the particles showed that particle borders were richer in vanadium than in iron compared to the particle centers (Table 5). In the same time, the smaller particles appeared systematically richer in vanadium than the larger ones. Both observations showed that the surface of the particles were richer in vanadium which correlates well with the XPS data. Enlargements of the micrographs showed that such surface enrichment did not bring any amorphization of the surface and that the particles are entirely crystallized (Fig. 3b). This tends also to confirm that vanadium entered the magnetite lattice and is not only supported on the magnetite.

The TPR profiles of the samples were similar, showing a small peak at 673 K and a larger one around 973 K (Fig. 4). According to a previous work [23], the first one was assigned to the formation of magnetite and the second to that of the metallic iron. In the present work, the first peak can be associated with the reduction of the surface, which was

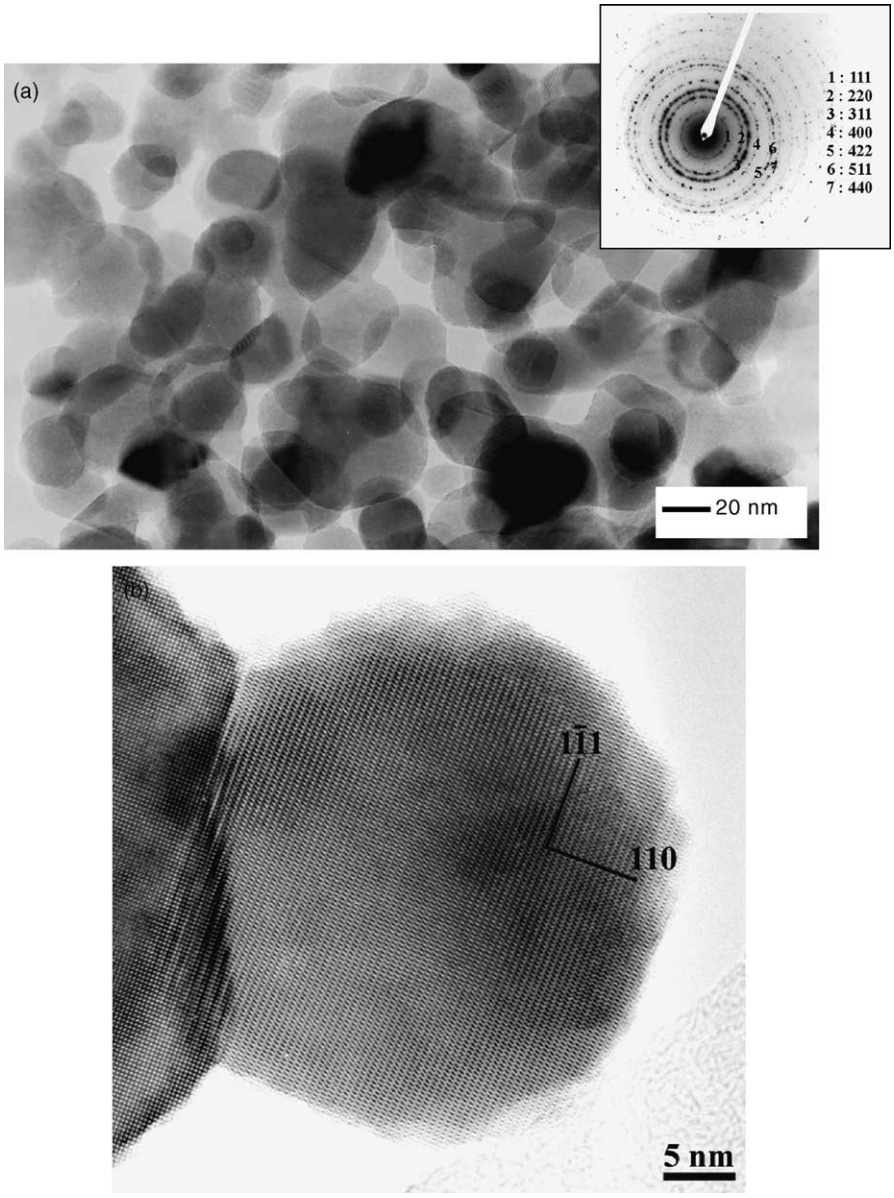

Fig. 3. (a) High resolution transmission electron micrographs of the V10 compounds with indexed electron diffraction patterns before the catalytic test. (b) Enlarged transmission electron micrographs of the V10 compound after the catalytic test showing the formation of necks between the particles and crystallized border of the particles.

partially oxidized when magnetite was exposed in air. The curves showed that vanadium delayed the formation of the metallic iron, since the reduction temperature of magnetite was shifted to higher values due to vanadium. As shown by electron diffraction, vanadium is distributed in the magnetite structure and then a contribution of V_2O_5 reduction is not expected. In addition the amount of vanadium is very slow and its reduction probably occurs simultaneously with iron reduction.

All catalysts were active in the HTS reaction as shown in Table 6. In the experiments carried out at $S/G = 0.6$, vanadium led to more active solids but the activity decreased as its concentration increased. At $S/G = 0.2$, the activity increased with the vanadium concentration.

The values of the activity per area showed that at low content (V/Fe = 0.03) vanadium acted more as a structural promoter rather than a textural one. At higher content its effect appeared to depend on the amount of steam; at *S/*

Table 5
Results of EDX analysis of the V10 compound (V/Fe = 0.10)

		V/Fe (molar)
Large particle center	Before the reaction	0.07 (1)
	After the reaction	0.08 (1)
Large particle border	Before the reaction	0.10 (1)
Small particle	Before the reaction	0.11 (2)
	After the reaction	0.12 (2)

Standard deviations for experimental values are given in parenthesis.

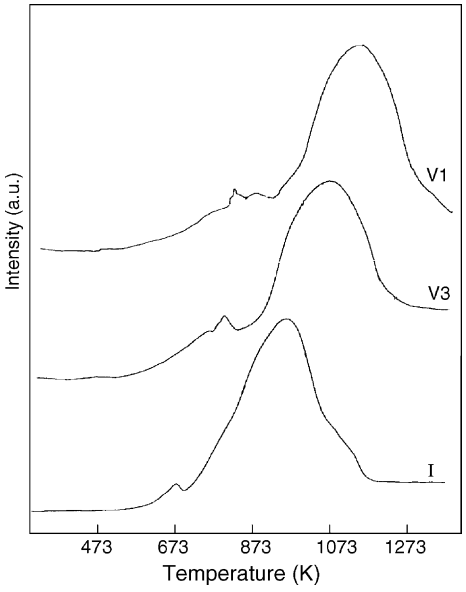

Fig. 4. TPR curves of pure magnetite (I sample) and vanadium-doped magnetite (V3 sample: V/Fe = 0.03; V10 sample: V/Fe = 0.1).

$G = 0.6$ vanadium increased the activity per surface area while at $S/G = 0.2$ it acted mainly as a textural promoter.

The mechanical mixture of pure magnetite (I sample) and vanadium oxide (V_2O_5) with a V/Fe = 0.1 showed an activity of 7.8×10^{-7} mol g^{-1} s^{-1} and a selectivity to carbon dioxide of 51%, under $S/G = 0.6$. The value of activity was lower than that observed with the V10 sample. In addition pure vanadium oxide did not show any activity in the same condition. Therefore, it can be concluded that vanadium acts as a structural promoter, changing the activity of the magnetite sites.

The action of vanadium in improving the activity can be explained by considering the regenerative mechanism, generally accepted for HTS reaction [2]. According to this mechanism, the surface undergoes successive oxidation and reduction cycles by oxygen and water and carbon monoxide, respectively, to form the corresponding hydrogen and carbon monoxide products:

$$CO_{(g)} + O_{(ads)} \rightleftarrows CO_{2(g)} + \square_O \quad (3)$$

$$H_2O_{(g)} + \square_O \rightleftarrows H_{2(g)} + O_{(ads)} \quad (4)$$

in which $\square_O$ is an oxygen vacant site. From the Mössbauer spectra it was seen that vanadium led to a more oxidized solid with cationic vacancies. The presence of the latter vacancies should change the rate of oxygen diffusion in the bulk of the solid or create sites of O_2 activation at the surface [24]. The re-oxidation mechanism, which is the rate determining step of the reaction, may involve O^- that has a greater mobility than O^{2-} from the lattice. In the pure magnetite, the reaction would only involve O^{2-} from the lattice.

The selectivity of the doped catalysts was higher than those of the plain solids and this effect increased with the amount of vanadium in the solids. The definition of selectivity, used in this work, considers the number of moles of carbon dioxide produced per number of moles of carbon monoxide that reacted. All catalysts showed higher selectivities in the presence of larger amounts of steam ($S/G = 0.6$), which means that less carbon monoxide went to hydrocarbon by the Fischer–Tropsch reaction [1]. From thermodynamics considerations, it is well known that in the HTS conditions the Fischer–Tropsch reaction may occur but it is significant only in the presence of metallic iron [1,2]. According to previous studies, our results can be explained by considering the role of steam in facilitating the reoxidizing of the metallic iron produced, during the reaction, which catalyze the hydrocarbon production [1,2]. As no metallic iron was detected in the solids, it is probable that it was produced during the reaction, but oxidized during or after the discharge of the reactor, as point out early [2]. It is well-known [1,2] that metallic iron can be produced under the WGSR and large amounts of steam must be used to avoid its formation.

Vanadium increased the selectivity and this can be assigned to its ability in preventing the metallic iron production, as shown in the TPR curves. The Fe(II)/Fe(III) ratios were close to those of fresh magnetite, showing that the catalysts were stable under the reaction atmosphere.

All samples were more active than a chromium-doped commercial catalyst (6.9×10^{-7} mol g^{-1} s^{-1}) under $S/G = 0.6$, indicating that the preparation method is a convenient way to get these catalysts. The vanadium-doped samples were much more active than the commercial sample, which means that vanadium is a promising dopant to HTS catalysts, when they are prepared in the active form. This dopant does not increase so much the specific surface

Table 6
Catalytic activity per gram (a) and per surface area unit (a/S_g), of catalyst, selectivity in the WGS reaction and the Fe(II)/Fe(III) ratio of magnetite (I sample) and vanadium-doped magnetite (V3 sample: V/Fe = 0.03; V10 sample: V/Fe = 0.1) after the reaction

Sample	$a \times 10^7$ (mol g^{-1} s^{-1})		$a/S_g \times 10^8$ (mol m^{-2} s^{-1})		Selectivity (%)		Fe(II)/Fe(III)	
	$S/G = 0.2$	$S/G = 0.6$	$S/G = 0.2$	$S/G = 0.6$	$S/G = 0.2$	$S/G = 0.6$	$S/G = 0.2$	$S/G = 0.6$
I	8.6	9.7	4.3	4.6	15	67	0.45	0.50
V3	14.2	17.2	5.5	6.2	26	82	0.47	0.50
V10	26.4	12.8	9.4	4.6	30	88	0.48	0.50
Com	–	6.9	–	–	–	80	–	–

area of the iron oxide, as it does chromium, but it is able to keep the area during the reaction. It also increases the intrinsic activity resulting in very active catalysts.

4. Conclusions

Vanadium-doped magnetite is produced by heating vanadium-doped iron(III)hydroxoacetate (IHA) under nitrogen. The solid is made off particles with different size and shapes with vanadium located mainly on the surface, as V(II) and V(IV) species. The particles, as well as their borders, have the structure of magnetite with vanadium species accommodated inside. The doping with vanadium led to magnetite richer in Fe(III) and with a higher specific surface area. The vanadium containing catalysts are more active than the pure one in HTS reaction and this is assigned to both textural and structural action. The first one is explained by the presence of vanadium on the surface or close to it, where it seems to keep the particles apart delaying sintering. The second one can be assigned to the role of vanadium in stabilizing more Fe(III) in the structure and thus favoring the successive oxidation and reduction cycles, during the reaction and avoiding the formation of metallic iron which cause the catalyst deactivation. The vanadium-doped catalysts were much more active than a chromium-doped commercial sample. Therefore vanadium is a promising dopant to HTS catalysts, which may prevent both the magnetite reduction and sintering during industrial processes ensuring thus longer life to the catalysts.

Acknowledgements

ILJ acknowledges to CNPq his graduate fellowship. This work was done by the grants from FINEP and CNPq.

References

[1] D.S. Newsome, Catal. Rev. 21 (1980) 275.
[2] L. Lloyd, D.E. Ridler, M.V. Twigg, in: M.V. Twigg (Ed.), Catalysis Handbook, Wolfe Scientific Books, London, 1996, p. 339.
[3] K. Kochloefl, in: G. Ertl (Ed.), Handbook of Heterogenous Catalysis, vol. 4, VCH, 1997, p. 1831.
[4] M. Lanieck, M. Malecka-Grycz, F. Domka, Appl. Catal. A: Gen. 196 (2000) 293.
[5] G. Doppler, A.X. Trautwein, H.M. Ziethen, E. Ambach, R. Lehnert, M.J. Sprague, Appl. Catal. 40 (1988) 119.
[6] J.L.R. Costa, S.G. Marchetti, M.C. Rangel, Catal. Today 77 (2002) 205.
[7] D.C. dos Santos, A.C. Oliveira, P.C. Morais, V.K.G., A.C. de Oliveira, M.L.S. Correa, M.C. Rangel, Stud. Surf. Sci. Catal., in press.
[8] J.M.T. Souza, M.C. Rangel, React. Kinet. Catal. Lett. 77 (2002) 29.
[9] H.E.L. Bomfim, A.C. Oliveira, M.C. Rangel, React. Kinet. Catal. Lett. 80 (2003) 359.
[10] J.M.T. Souza, M.C. Rangel, React. Kinet. Catal. Lett. 83 (2004) 93.
[11] A.I. Vogel, Quantitative Inorganic Analysis, Longman, London, 1961, p. 309.
[12] L. Häggström, H. Annersten, T. Erierson, R. Wäppling, W. Karner, S. Bjarman, Hyperfine Interact. 5 (1978) 201.
[13] File 83-1436. JCPDS-International Centre for Diffraction Data.
[14] P.S. Sidhu, R.J. Gilkes, M. Posner, J. Inorg. Nucl. Chem. 40 (1978) 429.
[15] A.E. Ringwood, Geochim. Cosmochim. Acta 7 (1955) 189.
[16] R.D. Shannon, C.T. Prewitt, Acta Crystallogr., Sect. B 25 (1969) 925.
[17] A. Styles, Catalyst Manufacture. Laboratory and Commercial Preparations, Dekker, New York, 1983, p. 117.
[18] J.L. Dorman, T. Meceron, P. Renaudin, V.A. Brabers, J. Phys. Collog. C1 41 (1980) 177.
[19] A.J. Koch, H.M. Fortuin, J.W. Geus, J. Catal. 96 (1985) 261.
[20] L. David, A.J.E. Welch, Trans. Faraday Soc. 52 (1952) 1642.
[21] G.C. Araújo, M.C. Rangel, Catal. Today 62 (2000) 201.
[22] C.D. Wagner, W.M. Riggs, L.E. Davis, J.F. Moulder, G.E. Muilenberg, Handbook of X-ray Photoelectron Spectroscopy, Perkin-Elmer, Eden Prairie, 1978, p. 76.
[23] J.C. Gonzalez, M.G. González, M.A. Laborde, N. Moreno, Appl. Catal. 20 (1986) 3.
[24] D. Kalló, in: Z.G. Szabó, D. Kalló (Eds.), Contact Catalysis, Elsevier, Amsterdam, 1976, p. 371.